ELECTRON COOLING RATES IN FNAL'S RECYCLER RING *

A. Shemyakin # and L.R. Prost
FNAL, Batavia, IL 60510, USA

Abstract

A 0.1-0.5 A, 4.3 MeV DC electron beam provides cooling of 8 GeV antiprotons in Fermilab's Recycler storage ring. The paper presents cooling rate formulas derived in the framework of a simple non-magnetized model and compares them with measurements.

INTRODUCTION

Since the first cooling demonstration in 2005 [1], the Recycler Electron Cooler (REC) is used for storing and preparing antiproton bunches for every Tevatron store. To understand and improve the cooling process, dedicated cooling measurements of two types are performed.

In drag rate measurements [2], a low-intensity, coasting antiproton beam is first deeply cooled. Then the electron energy is changed by a jump, and the evolution of the average antiproton momentum is analyzed.

In the measurements of the second type, an antiproton beam with a Gaussian velocity distribution is kept between barrier buckets at a constant length. After turning the electron beam on, the initial derivatives of the momentum spread and transverse emittance are recorded.

In this paper, we compare results of these measurements with a non- magnetized model.

COOLING MODEL

The REC employs a weak 105 G longitudinal magnetic field to focus the electron beam in the cooling section. The simplest model to estimate the cooling rates of the antiproton beam is as follows:

1. The influence of the magnetic field on the cooling dynamics is neglected (so-called non-magnetized cooling).
2. The electron beam properties are assumed to be the same along the cooling section and across the beam.
3. The angle and momentum distributions of both electron and antiproton beams are Gaussian.
4. Variation of the Coulomb logarithm L_c over the range of relative velocities is neglected, and it is taken out of the cooling force integral.
5. For both beams, velocity spreads in *x* and *y* directions are equal in the cooling section.
6. The antiproton beam is assumed to be coasting, i.e. effects of RF barriers are neglected.
7. Antiproton motion in all three directions is uncoupled.

Cooling force

Under these assumptions, the formula for the non-magnetized cooling force [3] can be reduced to a one-dimensional integral [4] (similar to what is called "Binney's formula" in [5]):

$$F_{b\_xi}(\vec{V}_p) = -A\cdot\frac{\partial}{\partial V_{xi}}U(V_{px},V_{py},V_{pz}),\ A = 4\pi\cdot m_e r_e^2 c^4 n_{eb}\eta\cdot L_c$$

$$U(V_{px},V_{pz},V_{pz}) = \frac{2}{\sqrt{\pi}}\cdot\int_0^\infty dt\frac{\exp\left(-\frac{t^2V_{px}^{\ 2}}{1+2\cdot\sigma_{ex}^2t^2}-\frac{t^2V_{py}^{\ 2}}{1+2\cdot\sigma_{ey}^2t^2}-\frac{t^2V_{pz}^{\ 2}}{1+2\cdot\sigma_{ez}^2t^2}\right)}{\sqrt{\left(1+2\cdot\sigma_{ex}^2t^2\right)\left(1+2\cdot\sigma_{ey}^2t^2\right)\left(1+2\cdot\sigma_{ez}^2t^2\right)}} \quad (1)$$

where F_{b_xi} , V_{pxi}, and σ_{exi} are the *xi* components of the cooling force, antiproton velocity, and electron r.m.s. velocity spread, correspondingly; n_{eb} is the electron density, m_e is the electron mass, r_e is the classical electron radius, *c* is the speed of light, η is the portion of the ring occupied by the cooling section. All values are in the beam frame.

Cooling rates

The beam-frame longitudinal cooling rate is derived by averaging the cooling force power over the antiproton velocity distribution $f_p(\vec{V}_p)$ [6]:

$$M_p\frac{d\sigma_{pz}}{dt_b}\sigma_{pz} = \int F_{b\_z}V_{pz}f_p(\vec{V}_p)\,d\vec{V}_p = \sqrt{\frac{2}{\pi}}\frac{A\cdot\sigma_{pz}^{\ 2}\cdot f_{long}(\alpha)}{\sqrt{\sigma_{ez}^{\ 2}+\sigma_{pz}^{\ 2}}(\sigma_{ex}^{\ 2}+\sigma_{px}^{\ 2})}, \quad (2)$$

$$f_{long}(\alpha) = \frac{1-\sqrt{\frac{\alpha}{1-\alpha}}\cdot\arccos(\sqrt{\alpha})}{1-\alpha},\quad \alpha = \frac{\sigma_{ez}^{\ 2}+\sigma_{pz}^{\ 2}}{\sigma_{ex}^{\ 2}+\sigma_{px}^{\ 2}},$$

where M_p is the proton mass, σ_{pxi} is the *xi* component of the antiproton r.m.s. velocity spread, and the case where $\sigma_{ex}=\sigma_{ey}, \sigma_{px}=\sigma_{py}$ is considered. Eq. (2) is valid for $\alpha<1$. This is typical for the REC parameters and will further be assumed in this paper. When $\alpha>1$, the result is expressed through $\cosh^{-1}(\sqrt{\alpha})$. In the lab frame, the time derivative of the momentum r.m.s. spread δp is calculated as

$$\delta\dot{p} \equiv \frac{\delta p}{\tau_{long}} \equiv \frac{d}{dt_l}\delta p = \frac{d\sigma_{pz}}{dt_b}M_p\,. \quad (3)$$

A similar integration for the transverse velocity gives

$$\frac{d}{dt_b}\left(\sigma_{px}^2\right) = \sqrt{\frac{2}{\pi}}\frac{A\cdot\sigma_{px}^2\cdot f_{tr}(\alpha)}{M_p(\sigma_{ex}^{\ 2}+\sigma_{px}^{\ 2})^{3/2}},$$
$$f_{tr}(\alpha) = \frac{\arccos\sqrt{\alpha}-\sqrt{\alpha(1-\alpha)}}{2(1-\alpha)^{3/2}}\,. \quad (4)$$

Eq. (4) takes into account a decrease of the cooling rate by a factor of 2 due to averaging over the betatron phases. Transition to the lab frame gives the expression for the time derivative of the transverse emittance:

$$\tau_{tr}^{\ -1} \equiv \frac{1}{\varepsilon}\frac{d\varepsilon}{dt_l} = \sqrt{\frac{2}{\pi}}\frac{A\cdot f_{tr}(\alpha)}{\gamma M_p(\sigma_{ex}^{\ 2}+\sigma_{px}^{\ 2})^{3/2}} \quad (5)$$

* FNAL is operated by Fermi Research Alliance, LLC under Contract No. DE-AC02-07CH11359 with the United States Department of Energy.
#shemyakin@fnal.gov

Note that the antiproton transverse velocities enter Eq. (3) and (5) only by being summed in squares with the transverse electron velocities. For REC operational parameters, typical velocity spreads in units of 10^7 cm/s are as follows: σ_{px} ~0.7–2, σ_{pz} ~0.7–1.5, σ_{ex} ~5, σ_{pz} ~0.2. For this range $\alpha << 1$, $\sigma_{ex}^2 >> \sigma_{pz}^2 >> \sigma_{ez}^2$ and Eq. (2)-(5) predict that the time derivative of the momentum spread and the logarithmic time derivative of the transverse emittance vary by less than by ±15%. The ratio of longitudinal and transverse cooling times τ_{long}/τ_{tr} from Eq. (3) and (5), which is a function of the single parameter α, is much less than 1.

Drag rate

In the drag rate measurements, the temporal evolution of the average antiproton momentum deviation $\overline{p} = \overline{P} - P_0$ is recorded after a change of the electron momentum to some value p_e. Here $\overline{P}$ and P_0 are the average and nominal momenta, correspondingly. To compare the rate $\dot{\overline{p}}$ with the model, the cooling force of Eq. (1) is integrated over a Gaussian antiproton velocity distribution and is transformed into the lab frame. Integration over transverse velocities yields to a compact formula [6]:

$$F_{lz}(\Delta p) = -F_0 \cdot \int_0^{\Delta p/p1} du \frac{e^{-u^2} u^2}{u^2 + \left(\frac{\Delta p}{p2}\right)^2} \qquad (6)$$

where $\Delta p = p - p_0$ is the offset of the antiproton momentum with respect to its new equilibrium value $p_0 = p_e \frac{M_p}{m_e}$, and

$$F_0 = \frac{n_{el}}{\vartheta_t^2} \cdot \frac{2}{\sqrt{\pi}} \cdot \frac{4\pi \cdot m_e r_e^2 c^2 \eta \cdot L_c}{\gamma^3 \beta^2}, \quad p1 = \delta W_e \cdot \sqrt{2} \frac{M_p}{\beta m_e c},$$

$$p2 = \vartheta_t \cdot \sqrt{2}\, \gamma^2 \beta c M_p, \quad \vartheta_t = \frac{1}{\gamma \beta c} \sqrt{\sigma_{ex}^2 + \sigma_{px}^2 - \sigma_{ez}^2},$$

$\vartheta_e = \frac{\sigma_{ex}}{\gamma \beta c}$ - 1D electron r.m.s. angle in the cooling section,

$\delta W_e = p_e \sigma_{ez}$ - r.m.s. ripple of the electron energy,

$n_{el} = \gamma\, n_{eb} = \frac{j_e}{\beta c}$ - electron density in the lab frame,

γ and β are the Lorentz- factors, and j_e is the electron current density. For a small momentum spread δp, averaging of the cooling force over the antiproton momentum distribution can be done by expanding the force near the average momentum offset:

$$\dot{\overline{p}} = \overline{F_{lz}(\Delta p)} \approx F_{lz}\left(\overline{\Delta p}\right) + F_{lz}''\left(\overline{\Delta p}\right) \cdot \frac{\delta p^2}{2}. \qquad (7)$$

Expansion (7) is converging when the contribution of the term with the second derivative is small. Therefore, an interpretation of a drag rate as a longitudinal cooling force, $\dot{\overline{p}} \approx F_{lz}\left(\overline{\Delta p}\right)$, is valid when

$$\delta p^2 << \frac{2 F_{lz}(\overline{p})}{F_{lz}''(\overline{p})}. \qquad (8)$$

A typical behavior of the second-derivative term $F_{lz}''\left(\overline{\Delta p}\right) \cdot \frac{\delta p^2}{2}$ is shown in Fig.1.

DRAG RATE MEASUREMENTS

In the drag rate measurements, usually only the initial slope $\dot{\overline{p}}$ immediately after the energy jump is used (see a detailed description in Ref. [7]). To provide enough information for fitting the curve $F_{lz}(\Delta p)$, the measurement is repeated at different jump amplitudes. In Ref. [7] these data were fitted to an approximation of Eq.(1) assuming zero transverse antiproton velocities. Fitting of the same data to Eq.(6) gives very similar values of the electron beam parameters θ_e, δW_e and j_e (Fig.1). It is related to the fact that antiproton transverse velocities enter Eq. (6) only through θ_t dominated by electron angles. Fig.1 shows that the condition of Eq. (8) was always fulfilled in these measurements.

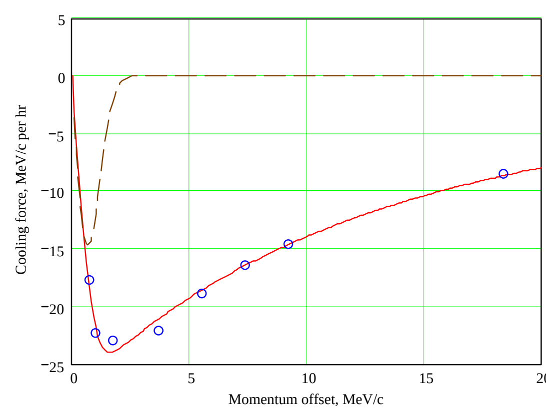

Figure 1. Drag rates measured on February 6, 2006 (blue circles). N_p = 3.5·10^{10} antiprotons, transverse emittance (95%, normalized, measured with a Schottky pickup) is $\varepsilon \approx$ 1.5π mm·mrad, initial momentum spread δp = 0.2 MeV/c, electron beam current I_e = 0.1 A. The red solid line represents Eq. (6) at δW_e = 370eV, θ_e = 0.2 mrad and j_e = 1.3 A/cm^2. Contribution of the second derivative term is shown by the dashed brown line (for presentation purpose, it is negated and shown for δp = 1 MeV/c). L_c = 10.

In addition, drag rate measurements were performed at a fixed amplitude of the energy jump while varying the electron beam current (Fig.2). The various data sets represent successive adjustments to the cooler, going from improving the alignment of the electron and antiproton beam trajectories after recalibration of the beam position monitors in the cooling section, to a novel beam-based alignment procedure of the cooling section magnetic field, to a new iteration of focusing setting optimization. Each time, the drag force increased, in particular for high beam currents and most notably for I_e = 300 mA. However, the reason for the drop at I_e = 400 mA is still unclear.

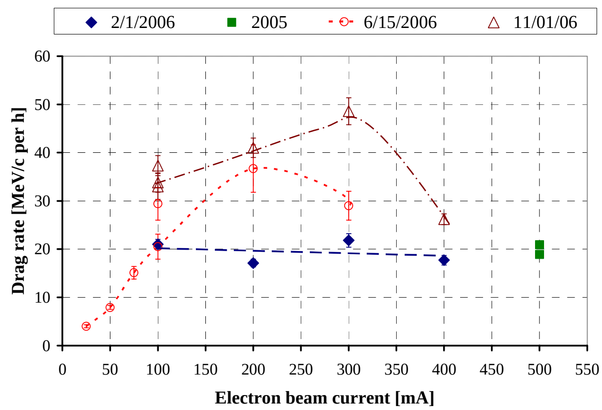

Figure 2. Drag rate (negated) as a function of the beam current. In all cases, the electron energy jump is 2 keV.

COOLING RATE MEASUREMENTS

An example of a cooling rate measurement is shown in Fig.3. An antiproton beam, kept between barrier buckets, is initially cooled only using the stochastic cooling system in order to create a velocity distribution close to Gaussian in all directions. The beam's momentum distribution is measured by a Schottky pickup, and the transverse distributions are measured with flying wires (FW). After turning off stochastic cooling, the antiproton beam is let diffuse. Then the electron beam is turned on. The difference of the slopes in the time of electron cooling and during diffusion is considered a measure of the cooling rate.

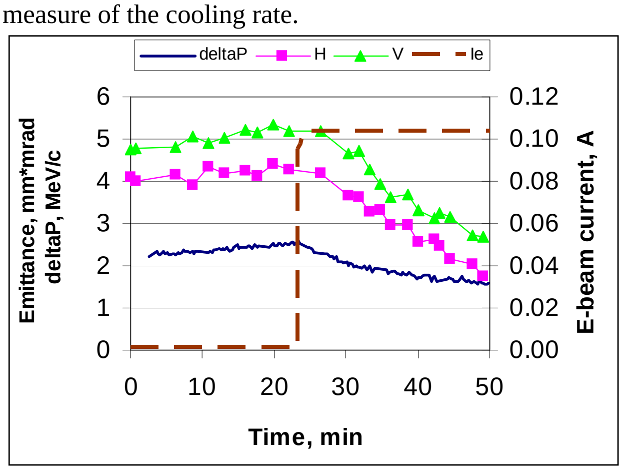

Figure 3. Cooling rate measurement (Dec 20, 2006). The beam length is 8.7 μs, $N_p = 50\cdot10^{10}$. The dashed brown line represents the electron beam current. H and V show the horizontal and vertical emittance (95%, norm., FW), respectively, and deltaP represents the r.m.s. momentum spread δp. The measured cooling rates are 8 (H), 11 (V) mm·mrad/hr, and 4.6 MeV/c per hr (δp), and corresponding cooling times are 0.52, 0.48, and 0.55 hours.

To compare the results with the model, the electron beam parameters found with the drag rate measurements shown in Fig.1 are fed into Eq. (2)-(5). The measured cooling rates are found to be consistently 2–3 times low for the longitudinal rate and high by a similar factor for the transverse rates. This results in τ_{long}/τ_{tr} ~1, which is also in disagreement with the model. So far no conclusive explanation for this discrepancy has been found. Several areas are looked into for hints:

- Instrumentation inconsistencies. For example, the transverse cooling rate recorded with a Schottky monitor is always significantly lower than the rate measured with flying wires [8].
- Heating mechanisms, including IBS.
- Dependence of the cooling rates on the antiproton emittance. Note that the drag force is always measured at a low emittance.
- Mechanisms of redistribution of the cooling rates, possibly similar to the one described in Ref. [9].
- Effect of the magnetic field on the cooling dynamics.

SUMMARY

1. In the framework of a simple model assuming Gaussian velocity distributions for the antiproton beam, formulas for electron cooling rates are expressed with elementary functions.
2. We find a significant disagreement (2-3 times) between measured cooling rates and predictions from our simple model combined with parameters fitted from the drag rate measurements.

ACKNOWLEDGMENTS

Authors are thankful to A. Burov, V. Lebedev, and S. Nagaitsev for many useful discussions. We acknowledge the participation of A. Fedotov and A. Sidorin in some of the measurements shown and the help from D. Broemmelsiek and M. Hu with instrumentation.

REFERENCES

[1] S. Nagaitsev *et al.*, Phys. Rev. Lett. **96**, 044801 (2006)
[2] H. Danared *et al.*, Phys. Rev. Lett. **72** (1994) 3775
[3] Ya.S. Derbenev and A.N. Skrinsky, Particle Accelerators **8** (1977) 1
[4] V. Lebedev, private communication
[5] I.N.Meshkov *et al.*, Physics guide of BETACOOL code, v.1.1, BNL note C-A/AP#262, p. 17
[6] A. Shemyakin, FERMILAB-TM-2374-AD
[7] L.Prost *et al.*, Proc. of HB2006, Tsukuba, Japan, May 29-June 2, 2006, WEAY02
[8] L.Prost *et al.*, Proc. of RuPAC'06, Novosibirsk, September 10-14, 2006, WEBO02
[9] M. Beutelspacher *et al.*, Proc. of EPAC'00, Vienna, 26-30 June 2000, p. 530